

Virtual Manufacturing as Tool for Material and Process Developments and Optimizations

Marcel Graf*, Sebastian Härtel, Carolin Binotsch, Birgit Awiszus

TU Chemnitz, Professorship of Virtual Production Engineering,
Chemnitz, Germany

*marcel.graf@mb.tu-chemnitz.de

ABSTRACT

Virtual process design based on numerical methods is a tool that has been widely used for years to help estimate expected forces, stresses and temperatures. Current efforts to improve hardware performance also seek to take account of the material itself in the numerical simulation. The necessary models to describe the material flow or microstructural development based on physical or semi-empirical approaches have been implemented to a large degree; however, the significance of the calculation results correlates strongly with the underlying material coefficients. These calculations are often based on the material data found in the reference literature or in material databases, as a process-specific material characterization would be time and cost intensive. There is usually no information about the method of determination (e.g., the type of flow curve), so the publicly accessible data is in principle only useful for an initial approximate calculation. The modelling constructed on the basis – forming behaviour and microstructural behaviour during the forming process – is the current research topic in numerous projects, with the intention of being able to draw conclusions about the mechanical properties in the final component after an FEM calculation. This should ultimately lead to processes and materials being optimized and modified in such a manner that, if the necessary component properties are known, a material-specific process route can be inversely deduced. This paper is intended to provide an overview of selected possible applications of FEM and to identify the potential benefits of having the corresponding material data of the forming blanks.

Keywords: numerical simulation, FEA, bulk forming, sheet forming, joining

Introduction

Everything from technological process stages up to entire process chains is increasingly being designed with the help of computer technology and related software tools. This makes a crucial contribution, particularly to environmental and resource conservation; however, a precise simulation requires appropriate models that accurately represent reality. Such models only provide sufficiently precise results when the thermophysical and forming-relevant material characteristics are available in full as input parameters. The continuous further development of the materials means that the determination of material-specific and forming-specific characteristics is also indispensable, as this is the only way to account for modern materials in detail in the simulation systems.

In order to achieve the objective of simulating closed process chains, it is imperative not only to take account of the influencing variables for describing the process, but also to consider the highly heterogeneous material properties within a process stage, as well as the material conditions that change along a process chain, when identifying the characteristics.

For this reason it is absolutely essential to adapt the material-specific determination of characteristics to the technological objectives, i.e., the specific forming processes, and to determine the increasingly important complex relationships and interactions between forming blanks and machinery through several process stages. Here, it is also necessary to ensure that the experimental simulation options take sufficiently precise account of the process under investigation with regard to forming speed, temperature, friction conditions, etc., in order then to provide this data for the numerical systems. In addition to the material characterization of the base material, another aspect that is increasingly gaining in importance is the description of the surface conditions (formation of oxidation products and their properties), as these phenomena affect both product quality and the overall material flow.

Material characterization

There are several experimental determination options available for characterising deformation behaviour. In principal, the analyses should focus on what the determination process is supposed to provide. Metallic materials are more sensitive to tensile stress than to compressive loads, for example, which means the forming capacity is manifested differently depending on the determination test. The more negative the proportion of hydrostatic stress (the non-forming portion), the greater the proportion of compressive stress, and the greater the capacity for forming without a material failure occurring in the form of cracks (Stenger diagram). However, each simulation should take equal account of the process-determining characteristics, so that recommendations can be derived with regard to the test procedure for the respective forming process. In order to account for any material anomalies, the dominant stress condition is the determining criterion. [1]

A further characteristic of the forming process being described is the strain rate, $\dot{\phi}$, which has an influence on the material properties and can be seriously divergent from one determination process to another. Another possible limiting process variable is the maximum achievable plastic strain ϕ , in the model test compared to the real process. Depending on which material-characterization options are available, the tensile test can provide an estimate of the deformation behaviour, but there are limits to its applicability, just as with the other test procedures.

One process variable that is gaining increasing attention is heating, which must also be taken into account in the experimental simulation. Industrial heating is tuned to the fastest possible heating depending on the component dimensions and material concept, whereby concepts based on induction and conduction are installed as well as convection- or radiation-based heating methods. The basic physical mechanisms for which the component and semi-finished-product temperatures are set and what heating speeds are used are therefore of huge importance. The heating can vary the solution condition of the alloying elements in the material. Also, depending on the heating modes, different temperature fields will form across the specimen cross-section and the specimen length; this has to be taken into account for the material characterization.

Phenomena concomitant to the process, such as friction, dissipated energy and necking, require corrective measures. The following two sections describe these measures for the respective test methods, as they are not universally applicable to the experimental simulation.

However, it is necessary to note that despite the use of comparison stresses for the uniaxial material characterization of the forming behaviour, differences may occur depending on the measuring procedure. These can happen for the following reasons:

- Deviating test approaches (with respect to specimen geometry, etc.);
- Defective measurands;
- Inaccuracy of the procedure for determining the comparison variable;
- Inhomogeneity of the stress and strain condition;
- Different modifications of the test temperature;
- Different frictional effects;
- Elastic yield of the test machines.

In practice, the use of database systems or values from reference literature, for example, has also become established. It bears mentioning that the determination procedure, the specimen position in the starting material, the initial microstructure and the evaluation procedure are usually only insufficiently known. As such, this material data can only be used for an estimate and not for process design, as the deviations from the material being used are not usually scalable. For this reason, it is advisable to perform a comprehensive characterization of the thermomechanical and thermophysical properties of the material itself.

Sheet forming processes

Deep drawing of bipolar plates

The low-temperature polymer-exchange-membrane fuel cells (LT-PEMFCs) used for the vehicle drive convert hydrogen, carried in tanks, into electricity, heat and water-vapour exhaust by reacting it with oxygen from the ambient air. An individual cell in its simplest form consists of a proton-conducting membrane electrode assembly (MEA), porous gas-diffusion layers (GDLs) and adjoining bipolar plates (BPs). Several individual cells in a stack are connected in series (Figure 1). Bipolar plates fulfil the following functions in the fuel-cell stack:

- Providing electrical contact between adjacent cells (bipolar anodes and cathodes)
- Supply and distribution of reaction gases, removal of products via channel structure in the flow field (Figure 1)
- Conduction, removal and supply of heat via internal cooling channels
- Separation of reaction gases of two adjacent cells
- Mechanical stabilization of the whole stack, support of the GDLs and MEA

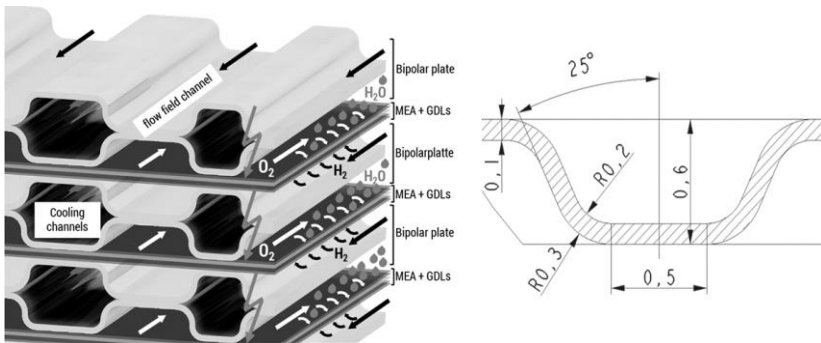


Figure 1: Cross-section of a fuel-cell stack (left) and formed channel (right)

Bipolar plates can consist of two formed halves joined together, which typically results in twice the number of individual sheets to be manufactured per fuel-cell stack. For example, a stack size of 370 cells¹ would require the production of more than 738 individual sheet metal plate halves per vehicle. This calls for cost-effective materials and production processes for bipolar plates that have the required properties: high electrical and thermal conductivity, very high corrosion resistance, mechanical strength, gas tightness with respect to hydrogen and low weight.

¹ Fuel-cell stack of the Toyota Mirai vehicle: 370 cells, system power $P_{\text{sys}} = 110 \text{ kW}$

To keep the cost of producing the bipolar plates as low as possible, the series-production process of deep drawing should be used. A functional research model was defined on the basis of state-of-the-art channel geometries for bipolar plates. Based on this model, a virtual tool was created in the form of a CAD drawing (see Figure 2, left) and finally transferred to a real tool (see Figure 2, right).

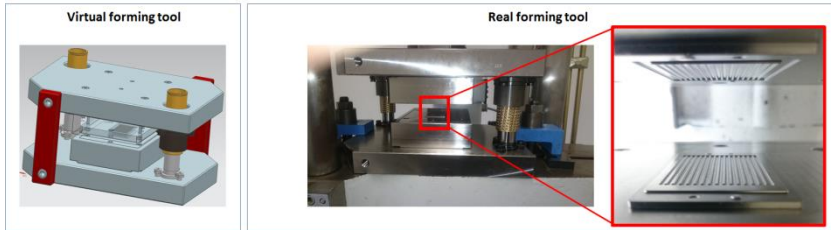


Figure 2: Virtual (left) and real tool (right) for the preliminary tests

In the preliminary tests of the functional research model, the components were first produced by deep drawing without hold-downs. All tests included continuous recording/measurement of the necessary process force, as well as the determination of the spring-back on the finished demonstrator component, in order to enable verification of the simulation based on these measurands.

Figure 3 shows the force curves determined experimentally with Galdabini and ZDTe machines as well as the curves determined numerically using volume and shell elements. It is evident from Figure 3 that the force curves determined numerically using volume as well as shell elements are highly correlative with the empirically determined force curve without elastic machine deflection (Galdabini test press).

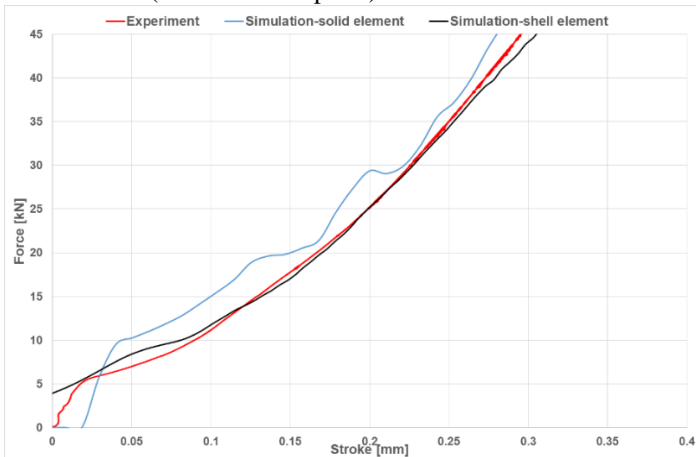


Figure 3: Force curves determined empirically and numerically when producing the functional research model

The simulation was verified not only by means of the force curves, but also based on the geometries arising after the deep drawing as well as the spring-back. Figure 4 shows the real geometry and the numerically calculated geometry (based on shell elements) after deep drawing. There is clearly a very good correlation between experiment and simulation with regard to the sheet indentation and the wrinkle geometry in the flange area.

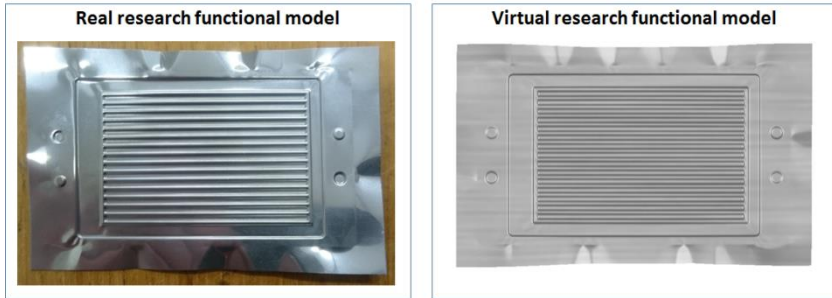


Figure 4: Real and virtual geometry of the functional research model after deep drawing

The spring-back evaluation variable was defined as the maximum difference in the deep-drawing direction, Δz_{\max} , at the outer edges of the sheet (see Figure 5, left). Here, too, there is a good correlation between experiment and simulation. The maximum measured difference in the z-direction is 5.9 mm and the maximum numerically determined difference is 5.5 mm. Thus, the difference between experiment and simulation is less than 10 %.

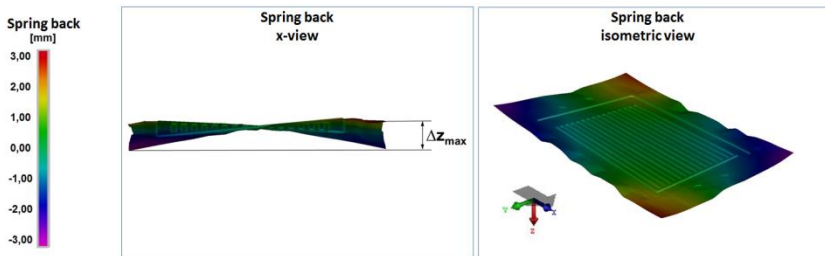


Figure 5: Numerically determined spring-back

Based on the demonstrably realistic FE simulation of the deep-drawing process on the functional research model, and using shell elements, the simulation model thus developed can be used to reduce wrinkling in the final bipolar plate. Taking this as a basis, the numerical calculation was extended to include a hold-down geometry that controls the material flow and exerts an additional contact pressure on free sheet surfaces. The film cross-section was increased to a size of 85 mm x 55 mm in order to produce a sufficiently large permanent contact surface between the film and blank

holder to eliminate wrinkling in the component-proximate areas. In summary, Figure 6 shows clearly that both wrinkling and spring-back following release of the drawn component were significantly reduced.

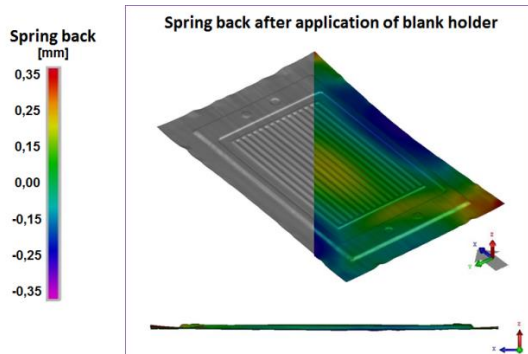


Figure 6: Reduction in spring-back achieved by adjusting the numerical calculation

Developing the non-circular spinning process

Metal spinning is defined by DIN 8584 as a process of sheet-metal forming with no intention to reduce the sheet's thickness. By applying forming techniques with a combination of tensile and compression conditions, a flat blank can be reshaped into almost any kind of rotationally symmetrical, hollow component, or alternatively, the form of such components can be changed. Sheet-metal spinning is an efficient and economical manufacturing process for the production of components in small- to medium-sized lots. Due to low tool costs (only one tool with the shape of the part is required), short set-up times and adaptable machine construction, spinning offers several advantages over conventional forming processes for small production lots, such as deep-drawing (see [2]). Moreover, it is possible to spin components with tight geometrical tolerances and to achieve a high-quality surface finish (see [3]). An opportunity to increase the economical relevance and flexibility of conventional metal spinning is the development of the process of "non-circular spinning" for producing rotationally asymmetrical components (see Figure 7).



Figure 7: Parts produced by conventional and non-circular spinning [4]

In principle, the production of rotationally asymmetrical, hollow components through spinning is possible with the application of force-controlled or motion-controlled roller tools (see Figure 8).

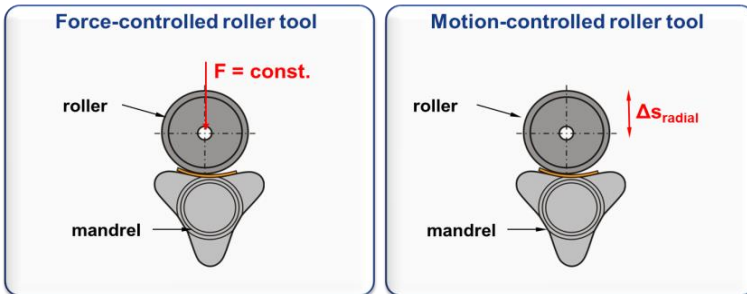


Figure 8: Principle of the force-controlled and motion-controlled rollers [5]

For the manufacturing of rotationally asymmetrical hollow parts through spinning the exact feeding of the roller tool in the axial and radial directions is necessary. This ensures a constant gap between the spinning mandrel and the roller at all times during the spinning process. The advantage of motion-controlled rollers in contrast to force-controlled rollers is that the former provide the possibility of actively influencing the resulting blank thickness, due to the constant gap between the mandrel and the roller. The motion-controlled roller method thus creates constant forming conditions in the concave and convex areas.

For the production of rotationally asymmetrical hollow parts, a spinning machine was developed according to the kinematical requirements for non-circular spinning with motion-controlled roller tools. The requirements are the supply of torque at the main spindle and the independent translational movement of the roller in the axial and radial directions. The non-circular spinning machine consists of two main parts, which can be seen in Figure 9:

- A main spindle as the drive component for the mandrel
- A two-axes table for radial and axial feed of the roller tool

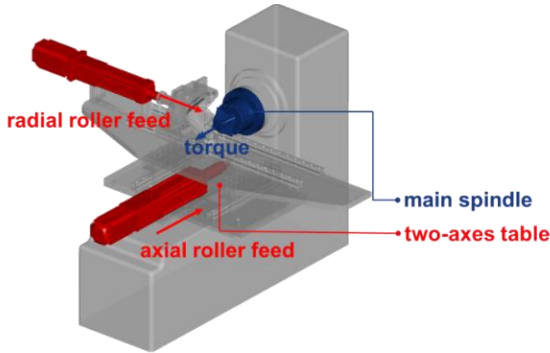


Figure 9: Main components of the non-circular spinning machine [4]

The roller tool is controlled by using a master/slave control, and the rotational axis of the main spindle is used as the master-axis. Therefore, the axial and radial movement of the roller tool (slave axis) is dependent on the actual angle of rotation of the main spindle. The advantage of this configuration is that rotational speed fluctuations do not influence the slave positions. An encoder measures the angle of rotation of the main spindle incrementally, and the roller tool is moved to the predefined slave positions. The non-circular spinning process is investigated experimentally using different mandrel shapes, as shown in Figure 10.



Figure 10: Mandrel shapes for non-circular spinning [4]

Härtel and Awiszus [6] performed experiments to determine the influence of the diameter of the blank, the roller feed rate and the operating angle of the roller on wrinkling and thinning.

The analysis of the experiments showed an increased tendency for wrinkling for greater initial blank diameters and higher roller feed rates. Moreover, for each part geometry, there is an optimal operating angle that leads to minimal wrinkling. Furthermore, the analysis of the sheet thickness showed that smaller initial blank diameters and higher roller feed rates lead to a reduction of sheet thinning – regardless of the part geometry. The operating angle also has a significant influence on sheet thinning when spinning the “Tripode” component. Here, a higher operating angle leads to reduced sheet thinning.

Nevertheless, it is possible to produce a wide range of geometries using the newly developed non-circular spinning process, as is shown in Figure 11. The component “Tripode” is characterized by a variation of concave and convex regions whereas the side walls of the component “Reuleaux” are convex and side walls of the component “Pagode” are concave.



Figure 11: Components produced by non-circular spinning [4]

To reduce wrinkling and thinning, the process was optimized using the Finite-Element Method (FEM). Thus, the development of thinning of wall thickness was analysed. The nodal result value for sheet thinning (in the critical thinning area) was determined as a function of the axial feed of the roller tool. The result for the development of sheet thinning is shown in Figure 12.

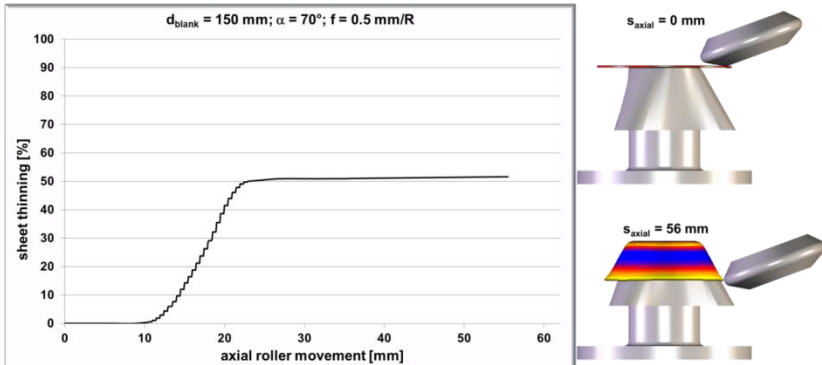


Figure 12: Sheet thinning depending on axial roller movement [7]

The numerical process analysis shows that a targeted variation of the roller feed rate and the operating angle during the process leads to minimized thinning and also minimized wrinkling. The investigations are shown in [7]. The roller feed rate during the non-circular spinning process can be varied within the existing machine and control concept. However, to swivel the roller tool during the process, a synchronous servo drive and a planetary gearbox have to be added to the existing machine concept. The integration of the synchronous servo drive and planetary gearbox within the existing machine configuration is shown in Figure 13.

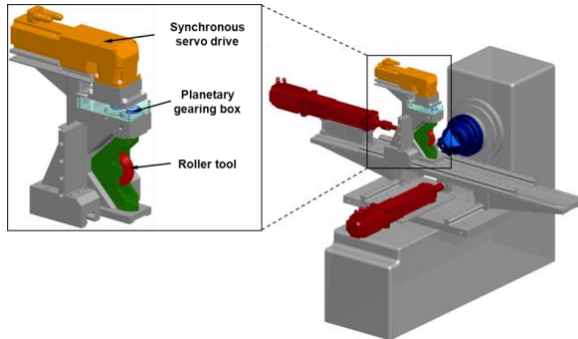


Figure 13: Integration of the swivel drive in the existing machine configuration [7]

The controlled variation of the roller feed rate and the operating angle during the process allowed the thinning to be reduced by up to 25 %.

Bulk forming processes

Forging of magnesium components

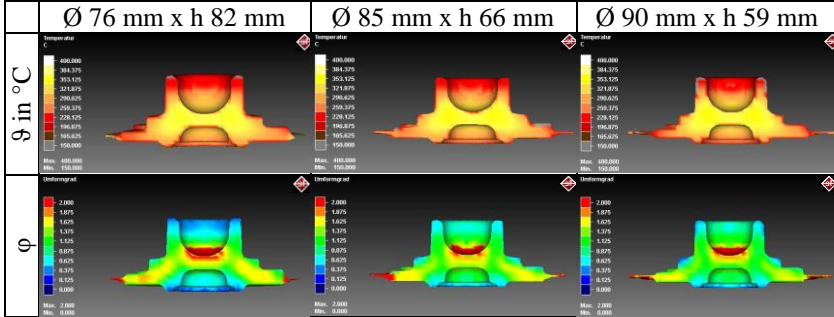
For the technological and material-oriented design of forged magnesium components, it is necessary to use a numerical simulation in which the determined material-specific variables are considered. It was the goal of the FEM to propose process parameters (including the necessary geometrical relationships) for the drop forging of a demonstrator component from AZ31 with different initial states, i.e., cast and extruded, and to validate these with subsequent forging tests.

The simulation focussed on the description of the microstructural features, as these are substantially responsible for the final properties of the components. The models required for this are based on the JMAK theory, whereby the process factors of temperature, local plastic strain and strain rate are of immense importance.

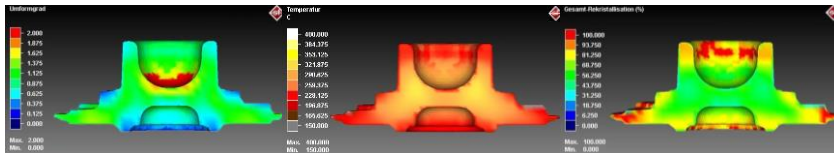
The process design was created to be of a practical nature with respect to the subsequent forging experiments, and for this reason the press speeds were varied (up to 40 mm/s) as they produce the strain rate, which exerts great influence on the hardening and softening behaviour. Another decisive parameter in ultimately achieving complete recrystallization of the microstructure is the plastic strain. Therefore, different initial diameters were used to produce different local strains. Because of their proportions (the ratio of height to diameter), care was taken to ensure that upon contact with the tool, the cylindrical original samples did not become unstable or buckle. It was also ensured that a sample height was selected that was not too large, so that the strain at fracture (maximum forming capacity) would not be exceeded by $\varphi_{\max} = 2.0$ [8]. In addition, the temperature profile in the test material can be controlled by the geometry, because the surfaces for heat

transfer differ. These relation-ships are depicted in Table 1 below for a magnesium sample at 450 °C that was forged to its final dimensions in a die at 200 °C with a tool speed of 10 mm/s.

Table 1: FE simulation with varied geometries [9]



It can be seen from this configuration how the process parameters influence each other and cause microstructural variations, and how inhomogeneously the different factors are distributed in the component. Taking an extruded cylindrical sample of Ø 90 mm × h 59 mm as an example, it can be shown (see Figure 14) that there are areas inside the hub that, due to the insufficient plastic strain, could not be transformed completely into a fine-grained, recrystallized microstructure with a starting temperature of 350 °C and a punch speed of 1 mm/s. Subsequent metallographic examinations verified the results of the simulation with respect to their accuracy.



a) plastic strain b) temperature c) RX fraction in %
 Figure 14: a) Adjusting effective (logarithmical) strain, b) temperature during forging of the wheel hub, and c) recrystallization distribution [9]

In Figure 15, the microstructure of the extruded AZ31 alloy is illustrated exemplarily under different conditions, whereby the forming was carried out once with an initial sample temperature of 350 °C at 1 mm/s and a second time with an initial sample temperature of 450 °C at 10 mm/s.

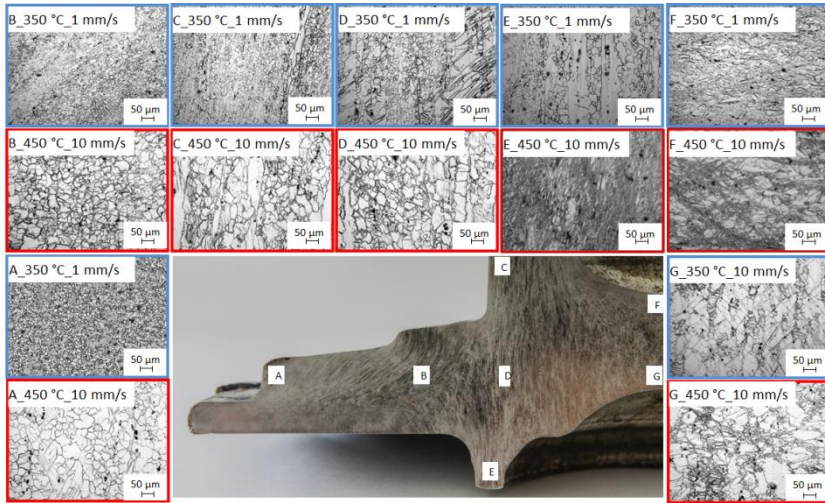


Figure 15: Microstructure in the wheel hub for 350 °C and 1 mm/s (blue frame) as well as for 450 °C and 10 mm/s (red frame) [9]

In accordance with the numerical simulation, the microstructural evolution (e.g., the grain size) depended to a significant degree on both the temperature and ram speed. The last Figure s show these dependencies exemplarily for the extruded magnesium alloy AZ31, considering several positions on the wheel hub. Due to the unequal distribution of the strain, different volume fractions of recrystallized grains were observed – complete recrystallization (e.g., A or B) and partial recrystallization (e.g., G). Areas of partial recrystallization were a result of insufficient strain, such that complete recrystallization could not occur. As expected, both grain size and volume fraction of the recrystallized grains increased with increasing temperatures. Higher temperatures adjusted the initiation and the completion of the recrystallization to lower strains. In addition, grain growth was promoted.

The biggest problem that magnesium alloys have is their susceptibility to corrosion, which is also the reason for the current hesitance in the adoption of magnesium in the forging industry. Current research is seeking ways of overcoming this problem by means of composite materials. In this way, for example, the coating of a magnesium sample with aluminium can make a significant contribution, which is explain in the next chapter.

Extrusion of aluminium magnesium compounds

The production of hybrid components from different materials is becoming increasingly important. Hybrid components not only have great potential for lightweight applications, but are also characterized by functional and stress-resistant designs. The use of magnesium or its alloys in particular can significantly reduce component weight due to their lower density compared

to other materials. Challenges related to the processing of magnesium are unfavourable flow properties and high susceptibility to corrosion.

In SRF 692 (Special Research Field “High-strength aluminium-based lightweight materials for security components”), research is being done in this regard to develop aluminium-coated magnesium materials that are produced by extrusion and then further processed into hybrid parts by means of additional forming processes such as upsetting, bending and forging. One objective of this research is to extend the currently limited fields of application for Mg materials as well as to permit applications in the same fields as for high-strength Al alloys but with more favourable material properties (low density). To this end, new machining and processing strategies are being developed for the novel material “Al-coated magnesium”, since the two materials are normally formed under different constraints.

Semi-finished products made from aluminium–magnesium composites are produced by hydrostatic extrusion. This process produces a rotationally symmetrical composite in which the aluminium encloses a magnesium core. In hydrostatic extrusion, the punch exerts a force on the billet and is pressed through the die. High plastic strain can be achieved thanks to the fluid friction of the hydrostatic medium between the billet and the recipient and the resulting improved lubrication conditions between the billet and the die. Hydrostatic extrusion also reduces tool wear and achieves improved surface geometry of the semi-finished product. [10]

In the process depicted, composites made from pure materials (aluminium and magnesium) as well as from alloyed materials (AlMgSi1 and AZ31) are produced. The initial outer diameter of the billet is 80 mm and the final diameter of the formed semi-finished product is 20 mm. Thus a plastic strain of approximately 2.7 is achieved. To ensure reliable processing of the difficult-to-form magnesium, the billet is preheated to 450 °C and the die to 350 °C. This activates further slip systems in the magnesium material, resulting in better formability. A billet with an initial length of approximately 300 mm produces an extrusion with a length of about 4000 mm (Figure 16).

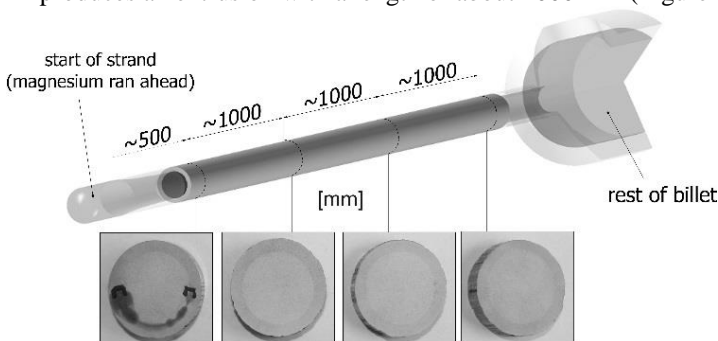


Figure 16: Composite quality, results of dye penetrant testing [10]

Parameter variations (tool and workpiece geometry, temperature, plastic strain, strain rate, etc.) were used to create a process window that enabled the production of a complete composite along the extrusion. By optimising the die geometry (angle and radii on the die shoulder) and the billet geometry, it was possible to improve the extrusion quality, with no cracking over the majority of the extrusion after achieving the quasi-stationary state [10]. Possible damage, such as cracking in the boundary layer, was checked for by means of penetrant tests (Figure 16).

The use of FEM provided significant support in achieving the goal of a stable process whereby semi-finished products can be produced with undamaged boundary layers between composite partners. The process was realistically modelled in 2D and 3D, simulated and investigated with various methods of analysis. The material flow and the deformation behaviour of the two materials were analysed in detail through additional modelling of sensors and flow lines (marking grids) in the FE system and through the evaluation of the different stresses.

Contact shear stress and axial difference of the plastic strain were identified as two scalable variables that demonstrate a relationship between their modification and the resulting quality in the extrusion. The statistical design-of-experiment (DoE) method was used and the many interactions of the process-influencing parameters were determined in order to allow better conclusions to be drawn with regard to extrusion quality. This led to the iterative optimization of the die and billet geometry, as it was possible to achieve consistent material flow of the different materials and thus significantly improve the extrusion quality.

The experimental results, together with the numerical analyses for the hydrostatic extrusion as well as the adhesive strength tests of the boundary layer, formed the basis for the creation of an integrative composite model. This model, based on empirical approaches, includes a quality model for predicting composite quality, an adhesive strength model to calculate composite strength and a diffusion model to calculate the interface thickness [11]. The adhesive strength model was implemented in the simulation by means of user subroutines, and so the interface strength is available as an additional evaluation variable in the post-processor.

Different metallographic and analytical tests (REM, EDX and RBA analyses) were used not only to determine the composite quality, but also to localize the phase areas formed during deformation and to identify the individual phases in their composition [12]. The hybrid composite AlMgSi1/AZ31 is characterized by the fact that a boundary layer consisting of the intermetallic phases Al_3Mg_2 (α -Al-Mg) and $Al_{12}Mg_{17}$ (γ -Al-Mg) is formed as a result of diffusion processes during extrusion (Figure 17). This interface exhibits very brittle behaviour and falls within the range of ceramic materials. Consequently, the challenge for further processing is whether this

brittle boundary layer is generally capable of further plastic deformation and how large the associated deformation capacity is.

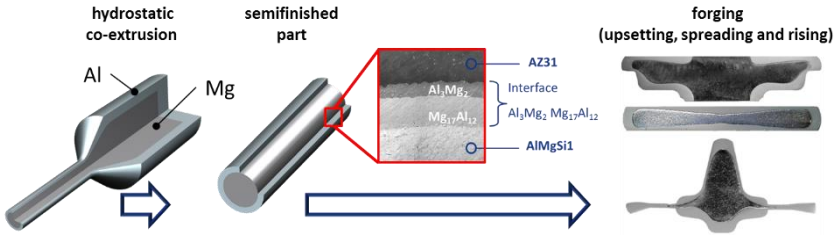


Figure 17: Process chain for production of Al–Mg compounds and the intermetallic phases after co-extrusion process [13]

Forging of lightweight hybrid components

The production of damage-free, extruded semi-finished products with subsequent forming into final components as a complete, high-strength composite results in diverse areas of application for lightweight construction. Such hybrid components can be used in the automotive sector, for example, as lightweight composite profiles for auto body assembly or as parts and components relating to the power train. There are further areas of application in rail-vehicle and aircraft construction, where a high percentage of load-bearing structural components are already made of lightweight profiles. Drop forging plays an important part in the further processing of extruded hybrid semi-finished products, as many automobile chassis components are produced via forging. All the more so as drop forging can be used to achieve high plastic strain and diverse shapes. The analysis of the deformation behaviour is carried out using the three different basic stress types – upsetting, spreading and rising – in order to better understand the complex forming processes and the behaviour of the boundary layer (Figure 18).

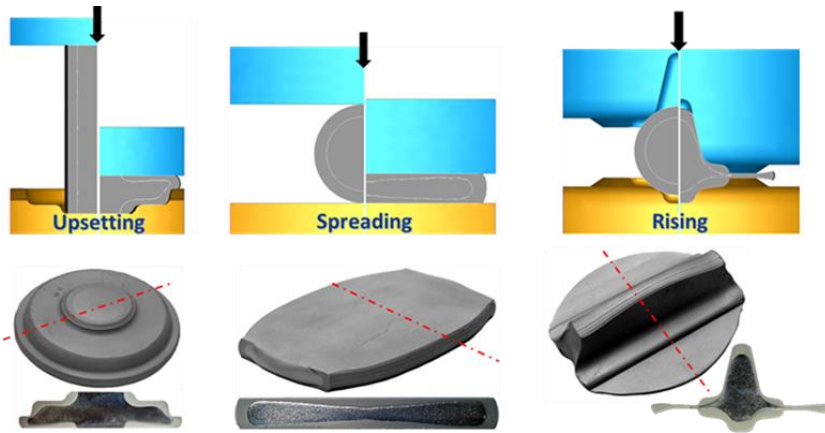


Figure 18: Schematic description of each forging process, (a) upsetting, (b) spreading, (c) rising and the real hybrid components [13]

The loading of the semi-finished product is primarily axial in the upsetting process and radial in the spreading process. In the rising process, the material flow is radial as well as tangential and also partially against the tool movement. The brittle boundary layer is thus subjected to strong compressive and tensile stresses. In Figure 18, it is clear in the cross-section of the actually forged components that a high deformation has taken place and the composite has remained visibly intact. The upsetting process shows that the axial load is non-critical and there is no damage to the boundary layer. Plastic deformation of the brittle intermetallic phases is possible, contingent on the direction of loading on the interface together with the hydrostatic pressure and the process conditions.

The spreading and rising processes cause a high level of stretching of the boundary layer, which results in the boundary layer breaking into several fragments (Figure 19). These fragments have typical characteristics such as length, thickness and twist direction, which in turn can be traced back to shear stresses by means of numerical methods. The areas between the fragments are fully closed. In the forming process, during fragmenting, there is also a welding of the composite materials as well as a diffusion process in which a new secondary boundary layer is formed [13]. This very thin new boundary layer (approx. 0.5 – 1.5 μm) consists exclusively of the $\gamma\text{-Al-Mg}$ phase and has been confirmed by materials analyses.

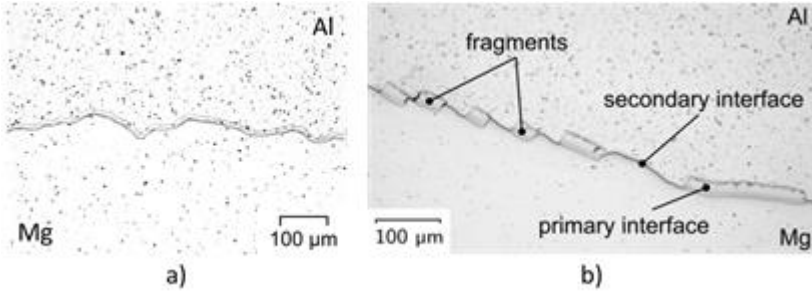


Figure 19: Rising process, metallographic analysis, (a) interface without cracks or fractures, (b) interface fragments with different sizes [13]

The determination regarding damage initiation in conjunction with the metallographic pictures demonstrated that fragmentation occurs even with small plastic strain. Fragmenting was even found in incremental tests with a forming displacement of 2 mm. This corresponds to a friction-free analytical comparison plastic strain of approximately $\varphi=0.1$.

The analysis for possible damage resulting from the metallographic testing showed that a complete composite was present between the two materials along the entire boundary layer, thus confirming that completely bonded semi-finished products also withstand high plastic strain during further processing. The prerequisite for this is complete bonding of the semi-finished products after extrusion. In pre-damaged semi-finished products or specimens joined via interference fit, no composite is produced, as both materials separate during the forming process. The boundary layer fragmentation that occurs in the case of certain loading directions is not problematic, because the firmly bonded composite remains intact due to the development of a new secondary boundary layer.

Based on the findings of the tests and analyses with regard to the phenomenological behaviour of the boundary layer, a complex component (SMART-Body) was developed which covers different mould elements (Figure 20) as well as all three basic forging types (upsetting, spreading and rising) during the forming process. After extrusion, the hybrid semi-finished product undergoes heading for mass pre-distribution; then, in the next process step, it undergoes final forging at a workpiece temperature of 300 °C and a forging die temperature of 200 °C. The high proportion of magnesium in the component interior reduced weight significantly. To protect the magnesium from corrosion in the case of corresponding burr formation, it is possible to completely encase the core with aluminium or, for open surfaces or functional surfaces such as bore holes, to apply a newly developed sol-gel coating.

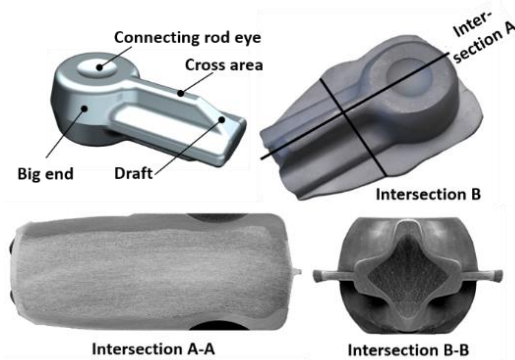


Figure 20: SMART-Body with intersections [14]

The novel process of eccentric extrusion was developed to optimize the preform and to reduce the thinning in certain areas of the protective aluminium shell, e.g., during rising. To this end, a defined offset (2 to 5 mm) is produced during the manufacture of the billet. The off-centre arrangement of the magnesium core is maintained throughout the extrusion process, thus producing an eccentric preform throughout the entire length of the extrusion (Figure 21).

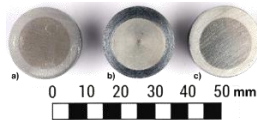


Figure 21: Semi-finished parts, (a) centric, (b/c) eccentric [15]

This displacement of the core material in the new eccentric extrusion process allows for greater design freedom, especially for asymmetrical forged components, and this makes it possible to provide the product development department with customized hybrid composites.

With respect to lightweight design, another idea was developed whereby a hybrid component made of an aluminium–plastic composite was produced for the first time by bulk forming. With the focus on lightweight constructions, the process line from the production of semi-finished products up to the second processing step of forging was investigated for composite of plastic (PA6) and aluminium alloy (EN-AW6060). In particular, the material or deformation behaviours were determined fundamentally. For analysing the temperature-dependent material flow, the three basic kinds of forging (upsetting, rising and spreading) were considered under laboratory conditions by using an oil-hydraulic forging press. The results show that the temperature profile over the cross-section of the composite and the ratio between aluminium and plastic is sensitive for the process stability and the forging of faultless components. Due to the decomposition temperature of the plastic, a

gradient temperature is necessary for the forging of hybrid plastic–metal composites. It must also be regarded that the diameter-height-ratio is important to eliminate the risk of buckling during upsetting. Additionally, the physical simulation takes into account for the identification of the process window for forging. The potential for weight reduction of the plastic-metal-hybrid is approximately 30 % higher in comparison to a monolithic aluminium component.

The challenge in the production of semi-finished products as well as in the further processing is essentially that the thermal stability of the aluminium alloy and the polyamide diverge very strongly (handling temperature of EN AW-6060 around 350 – 400 °C and of PA6 approximately 120 °C). Hence, a high gradient regarding to temperature over the cross section must be set up, but without melting or decomposing the plastic. Therefore, the heating processes of the different samples were different. The heating of aluminium tubes took place in an electrical chamber furnace up to 350 °C and a holding of 10 min after reaching the targeted temperature. The plastic component was not heated before joining. Subsequently, the monolithic raw materials were combined. As a result, the plastic heats up because of heat transfer from the aluminium to the PA6. Thus, the polyamide was heated only indirectly. Then the positioning of the semi-finished products in the dies followed. For determining the forming behaviour under real conditions all three basic forging processes (upsetting, spreading, rising corresponding to [13]) were examined. The difference between the processes is the position of the component axis to the load/deformation direction. For example, the process chain for upsetting is shown in Figure 22.



Figure 22: Process steps for the upsetting of hybrid aluminium-PA6 [16]

For the forming tests, the various dies were installed in an oil-hydraulic forging press with a maximum forming force of 1000 kN. All forging operations were carried out with a press speed of 80 mm/s. The minimum thickness of the flash gap was 2 mm. The joined aluminium plastic hybrids were positioned in the die and by using the heat from the production of the semi-finished product the forging process started. Because of heat transfer and heat flux of the aluminium tube the PA6 sample heated up to maximum 92 °C in the core, which was measured by thermocouples. Prior, the dies were lubricated with Lubrodal F25 AL from Fuchs Lubritech. Moreover, the dies always remained cold in order to realise a modified press

hardening in both materials after the forging process (closing time of the dies was 60 s).

The numerical analysis for the aluminium–plastic composite was carried out using Simufact.forming 13.03 and the PA6 material data (see [16]) both for the production of the semi-finished product and for the determination of suitable specimen-diameter ratios. In the first processing stage, the primary focus was on the elongation of the plastic as a result of heating by thermal conduction and on the mapping of the inhomogeneous temperature distribution across the cross-section, so that geometric as well as thermal boundary conditions are taken into account as pre-stages in the forging process. It is seen that the temperature of the PA6 in the contact area of the material pair rises to 180 °C and thus remains below the melting point ($\vartheta_{melting}=218\text{ °C}$). In the core, the temperature reaches approx. 85 °C (measured 92 °C) after a joining and handling time of 30 s. The simulation can even take account of the severe elongation of the plastic specimen that occurs in reality. In the subsequent upsetting, the influence of the wall thickness and the specimen height was tested in three scenarios ($d_{wall}= 2, 2.5$ and 5 mm) in relation to the aluminium tube. The use of plastic means the complete composite lacks interior stiffness, and this can lead to wrinkling during the upsetting process; for this reason, the specimen height of 35 mm proved to be suitable. The comparison between simulation and experiment showed good correspondence with respect to the production of the semi-finished product and the upsetting process (Figure 23).

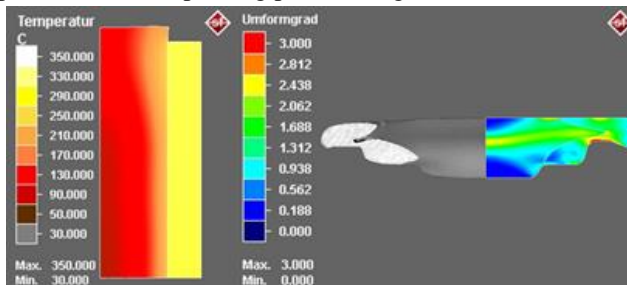


Figure 23: FEM of the heating of the hybrid semi-finished product and identical starting length (left; temperature) and the forging simulation and validation for upsetting (right; plastic strain); (not to scale between left and right) [16]

Joining technologies

Flat-Clinching

Flat-clinching is one process for the mechanical joining of metallic joining partners; this process is shown in detail in [17-19]. The functional principle of flat-clinching is shown in [17].

Because of its punctiform bonding geometry, the joint has no sealing effect. Therefore, flat-clinching cannot be used for applications that are intended for use with fluids or gaseous media (e.g., HVAC). Furthermore, when joining metals, there is a risk of moisture penetrating between the sheets and leading to corrosion. To create a seal between the two joining partners, adhesive must be applied before the joining process.

The combination of the mechanical joining (flat-clinching) and chemical joining (bonding) processes offers additional benefits beyond the sealing effect. On the one hand, the adhesive can be used to significantly increase the load capacity with respect to oscillatory and impact stress. On the other hand, flat-clinching can be used to support conventional adhesion processes. After the adhesive is applied, the sheets are joined by flat-clinching. Here, the mechanical joint serves primarily as a fixing aid until the adhesive is fully cured. This enables direct further processing of the component after joining and thus a significant reduction in process times. The final strength of the joint is achieved after the adhesive has fully cured.

During the forming process, the adhesive is displaced in the area of the direct joining zone, and this can result in the development of adhesive pockets (Figure 24). Reasons for this include excessively thick adhesive layers or unfavourably selected process parameters (e. g. hold-down forces, punch speeds, etc.) [19]. The development of large adhesive pockets can prevent the formation of an undercut, thereby significantly reducing the load-bearing capacity of the hybrid joint.

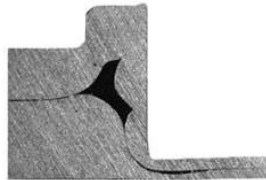


Figure 24: Adhesive pocket (black) after adhesive flat-clinching [18]

The numerical simulation was used to achieve optimal joint strength by means of adhesive flat-clinching, as described in [19].

Figure 25 shows the 2D axisymmetric model for the numerical simulation of adhesive flat-clinching. For reasons of visibility, the meshing of the adhesive is hidden. The materials used are DC04 with a sheet metal thickness of 1.0 mm (top sheet) and Al99.5 with a material thickness of 1.5 mm (bottom sheet). A layer of Betamate 1620 (thickness: 0.075 mm) is located between both metals.

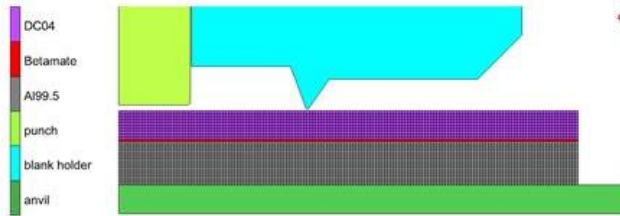


Figure 25: 2D axisymmetric simulation model of adhesive flat-clinching (Simufact.forming) [18]

All tools are defined as rigid bodies. The punch is defined as velocity-controlled (60 mm/sec, diameter: 5.0 mm, edge radius: 0.15 mm). Passive tools are the anvil and a blank holder with a v-ring contour (inner diameter: 5.1 mm, ring diameter: 13.1 mm, ring height: 1.1 mm). The blank holder load is implemented using a constant spring load. For the metal components, the material data are inserted into the FEM-software using the flow curves obtained in the plane strain compression tests. Furthermore, it is necessary to implement the viscoelastic flow behaviour of the adhesive, which is completely different from the flow behaviour of elastic/plastic metals. In contrast to metals, the flow curve of adhesives is characterized as a function of viscosity depending on the shear rate. Therefore, the viscosity of the adhesive was calculated by means of rheometer tests and subsequently implemented by means of the so-called Rate-Power-Law. The combined friction approach was chosen as physical model for the calculation of friction. For low contact stresses, coulomb friction is used, while shear friction is used for higher contact stresses.

Investigations revealed that it is possible to simulate adhesive flat-clinching. Figure 26 shows a visual comparison of the experiment and simulation for adhesive flat-clinching. It is clear that the joining point geometry and the adhesive distribution are well simulated, so the numerical model can be used for process optimization. Suitable optimization approaches are presented in [19].

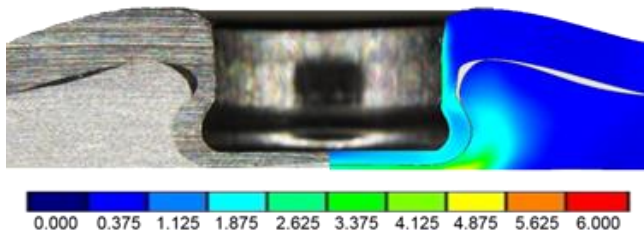


Figure 26: Adhesive flat-clinching: comparison of experiment and simulation (shown output value: total equivalent plastic strain) [19]

Metal inert gas welding of single- and multi-layers

On the one hand, the future promises a scientific analysis of the improvement in the component property when the weld seam is hot-formed using the welding heat. Initial results from numerical simulations show positive effects. Figure 27 show microstructural changes (grain refinement through recrystallization) and should ultimately result in improved mechanical properties.

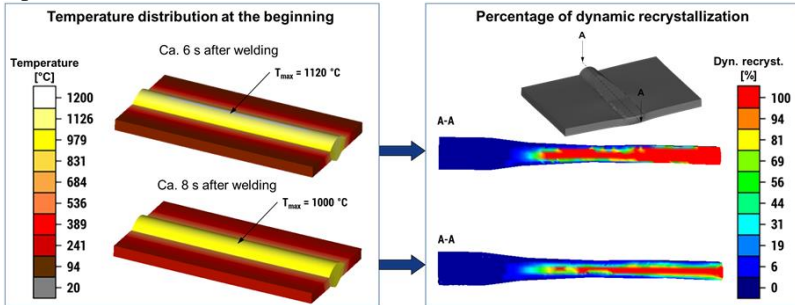


Figure 27: Recrystallization after hot-forming from the welding heat [20]

On the other hand, additive-manufacturing technologies have been gaining tremendously in popularity for some years in the production of single-part series with complex, close-to-final-contour geometries and the processing of special or hybrid materials. In principle, the processes can be subdivided into wire-based and powder-based processes in accordance with the Association of German Engineers (VDI) Guideline 3404. A further subdivision is made with respect to the smelting technology. In all of the processes, the base material is applied in layers at the points where it is needed in accordance with the final contour. This requires a repeated introduction of heat, which affects the microstructure of the components as well as the final mechanical properties. The components produced in this way should exhibit little warping or internal stresses as well as no porosity, so as not to negatively influence the usage properties. The objective is to reproduce these various technologies numerically in order to predict the component properties and, if applicable, determine the optimization potential.

The process that was investigated was wire-based, multi-pass welding by means of gas-metal arc welding, whereby the focus was on simulation and validation with respect to geometry and microstructural development in the weld passes. This was accomplished in the present case by determining all material parameters (mechanical and thermophysical) of the welding filler G4Si1 that were necessary for the numerical simulation and implementing them in a commercial FEM program (MSC Marc Mentat) (Figure 28).

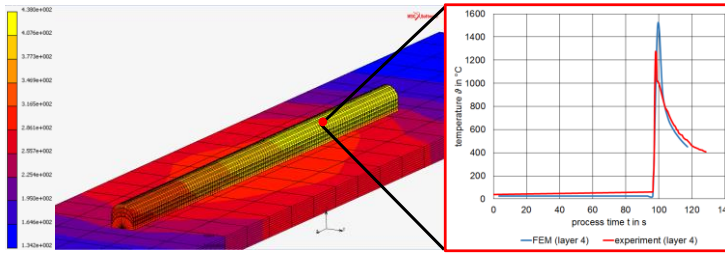


Figure 28: Temperature distribution after unidirectional welding of 4 layers and pause time of 15 s after each layer (welding direction: $-z$) [20]

The resulting minimal deviation between reality and simulation was a result of the measurement lag of the thermocouple. In general, however, the FE model can be used to make a very good predetermination of the cooling behaviour, which affects the microstructural development and thus the mechanical properties of the joining zone, as well as the geometric design of the component (distortion, etc.).

Conclusion

This paper provides an overview of the application of numerical simulation methods in the field of manufacturing technology to develop and optimize these and to analyze their process limits. However, it is state of the art to calculate the material flow with the resulting stresses and strains, but the numerical focus is now to describe the material evolution during the manufacturing processes. Thereby, on the knowledge of the microstructure changes along the process chain the mechanical properties (ductility, tensile strength, hardness, etc.) can be predicted. The FEA is meanwhile a standard tool for determining process limits, but the quality of the input parameters (especially material data, which must identify under process-relevant conditions, e. g. temperature, strain rate, plastic strain) has an essential influence on the calculation accuracy. Hence, the characterisation, material modelling and implementation of the temperature-dependent material data in the software in combination with experience for valuation of the numerical results and material behaviour can increase the benefit by using FEA.

References

- [1] Doege, E.; Behrens, B.-A.: Handbuch Umformtechnik; Berlin, Heidelberg, New York: Springer-Verlag, 2007, ISBN 978642042492.
- [2] Lange, K.: Umformtechnik – Handbuch für Industrie und Wissenschaft, Bd. 3: Blechbearbeitung; Berlin, Heidelberg, New York: Springer-Verlag, 1990, ISBN 3540500391.
- [3] Tschätsch, H.: Metal Forming Practise; Berlin, Heidelberg, New York: Springer-Verlag, 2005. ISBN 10354033216.

- [4] Härtel, S.; Awiszus, B.: Non-circular Spinning; In: Tekkaya, A. E.; Homberg, W.; Brosius, A.: 60 Excellent Inventions in Metal Forming, München: Springer Verlag, 2015, pp. 137 - 143.
- [5] Awiszus, B.; Härtel, S.: Numerical simulation of non-circular spinning: a rotationally non-symmetric spinning process; In: Production Engineering, 5(6), Springer Berlin/Heidelberg, 2011; doi:10.1007/s11740-011-0335-9.
- [6] Härtel, S.; Awiszus, B.: How to avoid wrinkling and cracking in non-circular spinning; Proceedings of MAPT 2012, 2012, pp. 48-53.
- [7] Härtel, S.; Laue, R.: An optimization approach in non-circular spinning; In: Journal of Materials Processing Technology, Volume 229, 2016, pp. 417-430.
- [8] Börnstein, R.; Landolt, H.: Numerical Data and Functional Relationships in Science and Technology; New Series / Editor in Chief: W. Martienssen, Springer Verlag, Berlin Heidelberg, 2011; ISBN 9783642138638.
- [9] Graf, M.; Ullmann, M.; Kawalla, R.: Property-oriented production of forged magnesium components; Materials Today: Proceedings 25 (2015), pp. 76-84.
- [10] Kittner, K.; Binotsch, C.; Awiszus, B.: Models for determination of interface strength and quality of aluminum-magnesium compounds; steel research international, Vol. 81 (2010), No. 9, pp. 454 – 457, ISBN 9783514007741.
- [11] Kittner, K.: Integrativer Modellansatz bei der Co-Extrusion von Aluminium-Magnesium-Verbunden; PhD-Thesis, TU Chemnitz, 2012.
- [12] Kittner, K.; Awiszus, B.: The Process of Co-extrusion – An Analysis; Key Engineering Materials, Vol. 491 (2011), pp. 81 – 88.
- [13] Binotsch, C.; Nickel, D.; Feuerhack, A.; Awiszus, B.: Forging of Al-Mg Compounds and Characterization of Interface; Procedia Engineering Volume 81, pp. 540–545.
<http://www.sciencedirect.com/science/article/pii/S1877705814013083#>.
- [14] Förster, W.; Binotsch, C.; Awiszus, B.; Dietrich, D.; Nickel, D.: Interface engineering of aluminum-magnesium compounds; Materials Today: Proceedings 2S (2015), pp. 3 – 8; doi: 10.1016/j.matpr.2015.05.002.
- [15] Förster, W.; Binotsch, C.; Awiszus, B.; Lehmann, T.; Müller, J.; Kirbach, C.; Stockmann, M.; Ihlemann, J.: Forging of eccentric co-extruded Al-Mg compounds and analysis of the interface strength; IOP Conference Series: Materials Science and Engineering, Vol. 118; 12032; <http://iopscience.iop.org/1757-899X/118/1/012032>.
- [16] Graf, M.; Härtel, S.; Binotsch, C.; Awiszus, B.: Forging of Lightweight Hybrid Metallic-Plastic Components; Procedia Engineering 184 (2017), pp. 497 – 505; doi: 10.1016/j.proeng.2017.04.120.

- [17] Gerstmann, T.; Awiszus, B.: Recent developments in flat-clinching; *Journal of Computational Materials Science*, Vol 81, 2014, pp. 39 – 44, <http://dx.doi.org/10.1016/j.commatsci.2013.07.013>.
- [18] Gerstmann, T.; Lüder, S.; Awiszus, B.: Development of hybrid flat-clinching based on numerical simulation; *Proceedings SFU 2014*, 2014, pp. 80 – 87; ISBN: 9783860124901.
- [19] Gerstmann, T.: Erweiterung der Verfahrensgrenzen des Flach-Clinchens; PhD-Thesis, TU Chemnitz, 2016.
- [20] Graf, M.; Härtel, S.; Hälsig, A.: Numerische Auslegung des Mehrlagenschweißens als additives Fertigungsverfahren; 9. SAXSIM, Chemnitz: Universitätsverlag Chemnitz, 2017; ISBN 9783961000111.